JOURNAL OF MATERIALS SCIENCE 28 (1993) 4681–4688

Temperature dependence of the elastic moduli, dilational and shear internal frictions and acoustic wave velocity for alumina, (Y)TZP and β′-sialon ceramics

M. FUKUHARA
Toshiba Tungaloy, Technical Research Laboratory, 1-7, Tsukagoshi, Saiwai-Ku, Kawasaki, 210, Japan

I. YAMAUCHI
Cho-onpa Kogyo, Technical Engineering Department, 1-6-1, Kashiwa-Cho, Tachikawa, Tokyo, 190, Japan

Young's, shear and bulk moduli, Poisson's ratio and Lamé parameters, longitudinal and transverse internal friction values and acoustic wave velocity anisotropy factors for three kinds of polycrystalline compounds, α-alumina, yttria-stabilized tetragonal zirconia polycrystal, (Y)TZP, and β′-sialon, $(Si,Al)_3(N,O)_4$, were simultaneously measured over a temperature range 295–1773 K, by an ultrasonic pulse sing-around method. These elastic moduli and Lamé parameters decreases and Poisson's ratio increases with increasing temperature, suggesting activation of a shear mode in the high-temperature region. The high-temperature shear internal friction for (Y)TZP and sialon were more sensitive to relief of strain and softening of glassy phase at grain boundaries, respectively, compared with the dilational friction.

1. Introduction

It is well known that elastic constants as well as dielectric constants are important material parameters for evaluation and design of materials. A few high-temperature elastic data for high-temperature structural materials such as silicon nitride [1–3], silicon carbide [3, 4], alumina [2, 5–7], zirconia [2, 3, 5] and silica [8] have been reported for their respective elastic parameters, mainly Young's modulus, but no research work has been carried out on simultaneous measurement of various elastic parameters from room temperature to high temperatures up to 1773 K. In particular, simultaneous measurement of both Young's and shear moduli makes calculation of Poisson's ratio and Lamé constants possible. (Lamé constants in isotropic solids are generally defined by two elastic constants, C_{12} ($= \lambda$), C_{44} ($= G$) in the elastic constant matrix which is composed of six rows and six columns. In this study, the Lamé constant is limited to λ.) The Poisson's ratio of ceramics has generally been treated as a constant in the high-temperature region, although Carnevale *et al.* [8] and Ryshkewitch [9] have reported that elevated-temperature values of alumina and silica, respectively, are somewhat higher. Insufficient attention has been paid to Lamé parameters at elevated temperature. (Strictly speaking, because Lamé constants are a function of temperature, "Lamé parameter" is used in place of "Lamé constant" in this study.) If these parameters are available up to high temperature, high-temperature materials could be precisely designed for advanced structural and functional application with high reliability.

Since the pioneering works of internal friction in polycrystalline metals by Zener [10] and Kê [11], the internal friction for polycrystalline ceramics has been measured in alumina [2, 6, 7], zirconia [2, 3, 12], silicon nitride [2, 3, 13, 14] and silicon carbide [3] by the flexural resonant frequency method [15] up to elevated temperature. However, high-temperature simultaneous measurement of internal friction values by longitudinal and transverse vibration modes has not been reported as far as we know.

In this study, Young's, shear and bulk moduli, Poisson's ratio and Lamé parameter, longitudinal and transverse internal friction values and acoustic wave velocity anisotropy factors for three kinds of polycrystalline compounds, α-alumina, yttria-stabilized tetragonal zirconia polycrystal, (Y)TZP, and β′-sialon are spontaneously measured over the temperature range 295–1773 K, by an ultrasonic pulse sing-around method. It is known that a pulse method of measuring the velocity of sound in solids is a sensitive indication of physical and structural changes [16]. Temperature dependence of acoustic properties for the materials is discussed in view of phase transformation, deformation mode, softening of the grain-boundary phase and

0022–2461

diffusion of ions, because high-temperature strength effectively depends on material structure [17] and residual stress [18].

High-temperature measurements of Young's and shear moduli have mainly been carried out by flexural vibration [12] and resonance frequency methods [2, 3, 6, 7, 14, 15]. However, these methods have many disadvantages, such as uncertainty of dimensionality in flexural or torsion resonance, high-frequency fatigue under applied stress [19], adjustment of suspension position [15], exfoliation or deterioration of coated electrical film on the sample. In contrast, the pulse method is suitable for high temperatures when internal damping makes the resonant method very difficult [16]. In particular, the ultrasonic pulse sing-around method with zero cross time detection and multiple delay circuits is still more suitable for accurate measurement.

2. Experimental procedure

Some properties of three kinds of polycrystalline ceramics used in this study are listed in Table I. All elastic moduli and internal friction values were accurately measured in argon at ambient pressure by means of the ultrasonic pulse sing-around method [20, 21] with zero cross time detection and multiple delay circuits, since "main" and "trailing" signals always overlap in the propagation of spurious echoes. The time detection and delay circuits are characterized by reducing errors due to fluctuation of the receiving pulse pattern and by preventing errors due to interference of multi-echoes, respectively. The apparatus and the specimen are schematically shown in Fig. 1a and b, respectively. The specimen was in the form of a long rod (20 mm long) united by a buffer rod (waveguide) with threads of pitch 1.5 mm, to eliminate the generation of spurious signals by mode conversion at the sides [22, 23]. Because the main and trailing pulses interfere especially when the waveguide has a small diameter [24], a specimen with 12 mm diameter was selected. A thermocouple was placed in a hole near the circumference of the specimen at the shoulder side.

The specimens, which were vertically mounted in an infrared heating furnace, were heated at a rate of 0.8 K s^{-1} and held for 45–90 s, when the sound velocity equilibrated within 0.5 % allowance, at 50 K intervals up to 1773 K. Precise measurement for alumina and (Y)TZP could not be made in the cooling run accompanied by the occurrence of cracks. However, all behaviour during the cooling process resembles that in the heating run. In order to avoid propagation loss due to high ultrasonic frequency, actually depending on frequency or the square of frequency [25], a frequency of 5 MHz was selected. The water jacket at the bottom of the rod cooled it so that the longitudinal wave generation PZT transducer at the bottom end was kept at room temperature. The smaller diameter section which was in the hot zone of the furnace, was the index region in which the transit-time measurements were made. Because trailing pulses are generated when a longitudinal sound wave is propagating into a rod, both longitudinal and shear velocities were determined in one run [22, 23].

The elastic behaviour of materials is characterized by two parameters, shear modulus, G, and the Lamé parameter, λ. The longitudinal modulus C and the shear modulus are related to the speed of longitudinal and transverse sound waves V_l and V_s by

$$C = \lambda + 2G = \rho V_l^2 \quad (1)$$

$$G = \rho V_s^2 \quad (2)$$

where ρ is the specimen density. Young's modulus, E, bulk modulus, K, and Poisson's ratio, ν, can be calculated from G and C using the elasticity parameter formulae

$$E = \frac{3C - 4G}{C - G} G = \frac{3\lambda + 2G}{\lambda + G} G \quad (3)$$

$$K = C - \frac{4}{3} G = \frac{\lambda + 2G}{3} \quad (4)$$

$$\nu = \frac{1}{2} \frac{C - 2G}{C - G} = \frac{\lambda}{2(\lambda + G)} \quad (5)$$

Increasing rates in the internal friction ΔQ_{lt}^{-1} and ΔQ_{st}^{-1} at temperature t were calculated from Equations A11 and A17 in the Appendix.

3. Results

3.1. Temperature dependence of elastic moduli

Young's, shear and bulk moduli, Poisson's ratio and

TABLE I Some properties of three kinds of polycrystalline α-alumina, (Y)TZP and β′-sialon ceramics

Material	Density ($Mg\ m^{-3}$)	Hardness			Transverse rupture strength, 298 K		Fracture toughness ($MN\ m^{-3/2}$) 298 K	Thermal expansion ($10^{-6}\ K^{-1}$)	Thermal conductivity ($W\ m^{-1}\ K^{-1}$) 298 K
		HRA	H_v		Mean value (MPa)	Weibul modulus			
		298 K	298 K	1273 K					
α-alumina	3.98	93.9	2040	710	490	6	3.3	7.9	12.4
(Y)TZP	6.05	91.3	1340	60	1400	17	9.8	9.2	7.9
β′-sialon	3.27	92.6	1600	1100	930	9	7.0	3.6	14.3

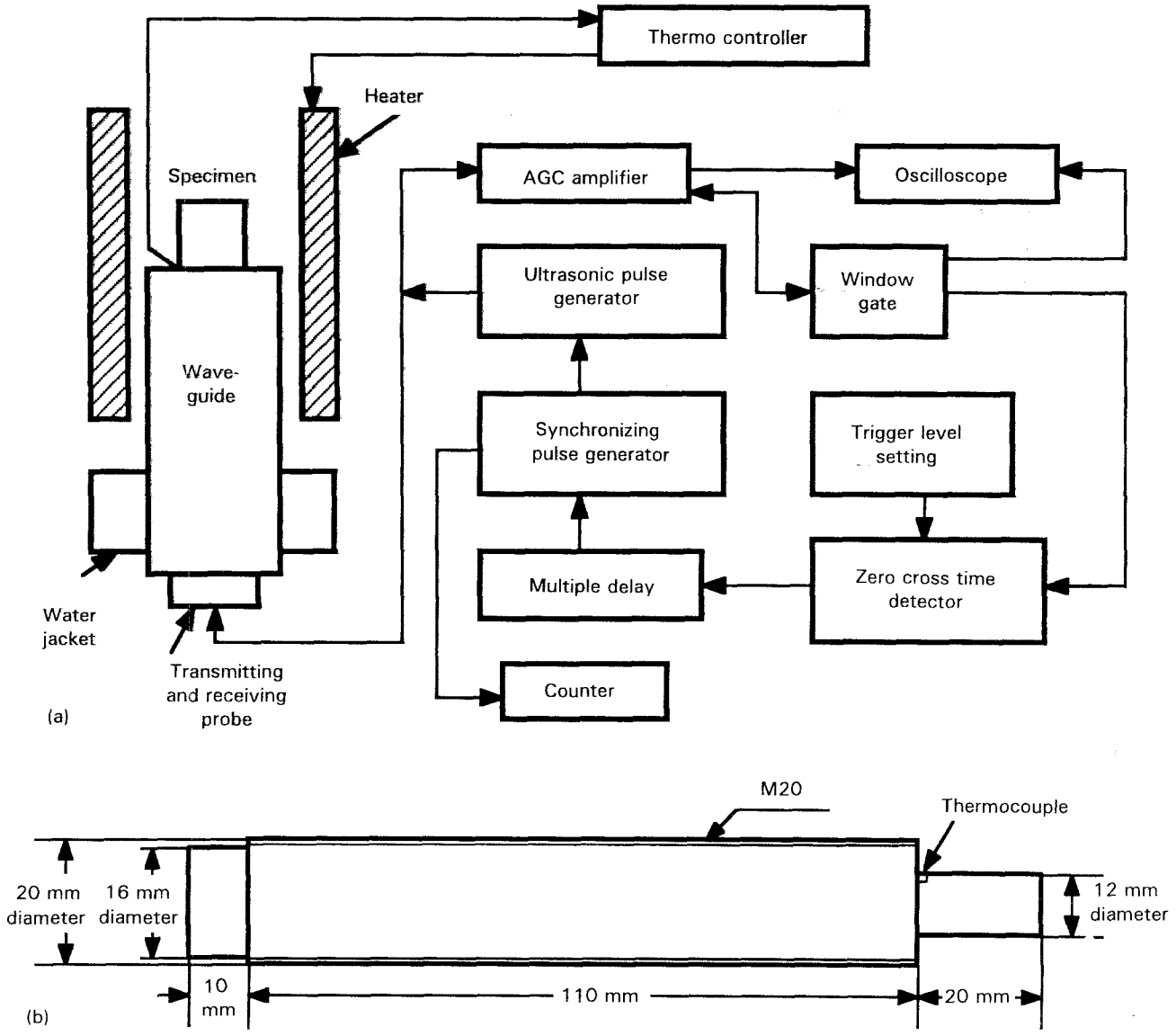

Figure 1 (a) Block diagram of apparatus for dynamic measurement of elastic parameters and internal friction, and (b) schematic diagram of specimen united by buffer rod with threads of pitch 1.5 mm.

Lamé parameter of α-alumina ceramic as a function of temperature are shown in Fig. 2a–c. The three moduli decrease substantially, while Poisson's ratio increases, as temperature increases. The room-temperature value of Young's modulus is consistent with data of polycrystalline alumina [8], but the modulus–temperature slope is smaller than other data [2, 6, 7]. Shear modulus values are larger over the whole temperature range in comparison with the data (123 GPa at 315 K and 39 GPa at 1800 K) reported by Ryshkewitch [9]. The increase in Poisson's ratio is more sluggish compared with the data up to 1089 K [9]. The Lamé parameter increases abruptly from about 1480 K with increasing temperature. This apparently suggests inactivity of the shear mode.

The temperature dependence of elastic moduli in (Y)TZP is presented in Fig. 3a–c. The dependence of the three elastic moduli and Poisson's ratio in (Y)TZP resembles that of alumina, except for a jump from around 1673 K. This jump would be due to the strain point [26]. Young's modulus of (Y)TZP at room temperature is almost the same as data reported by Sakaguchi *et al.* [3], whereas the degree of decrease in the high-temperature range is smaller than their data. Shear modulus at room temperature is consistent with the data of unstabilized zirconia [27]. The effect of temperature on the shear modulus of (Y)TZP has not been reported as far as we know. In contrast, the Lamé parameter decreased with increasing temperature, accompanied by a small broad peak at around 950 K and a jump at around 1673 K. The peak seems to be connected with internal frictions as described later. The decrease over the whole temperature range suggests activation of the shear mode.

Fig. 4a–c show the three moduli, Poisson's ratio and Lamé parameter as a function of temperature for the β′-sialon ceramic. The three temperature-dependent moduli reveal a distinct decrease up to around 1600 K. Poisson's ratio gradually decreases with increasing temperature, but shows one peak at around 1703 K. The Lamé parameter decreases suddenly from around 1625 K, after a sluggish decrease. It is considered that this behaviour in sialon is related to the existence of binder phases consisting of oxides.

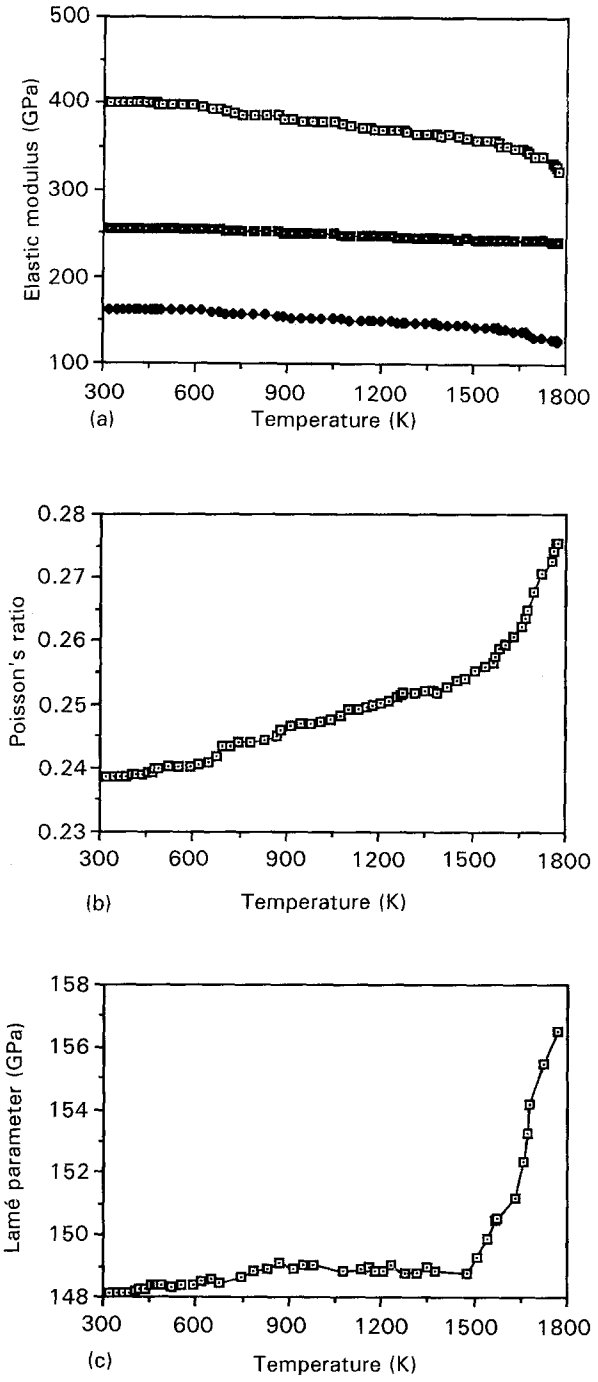

Figure 2 (a) (□) Young's, (◆) shear and (■) bulk moduli, (b) Poisson's ratio, and (c) Lamé parameter, of α-alumina as a function of temperature.

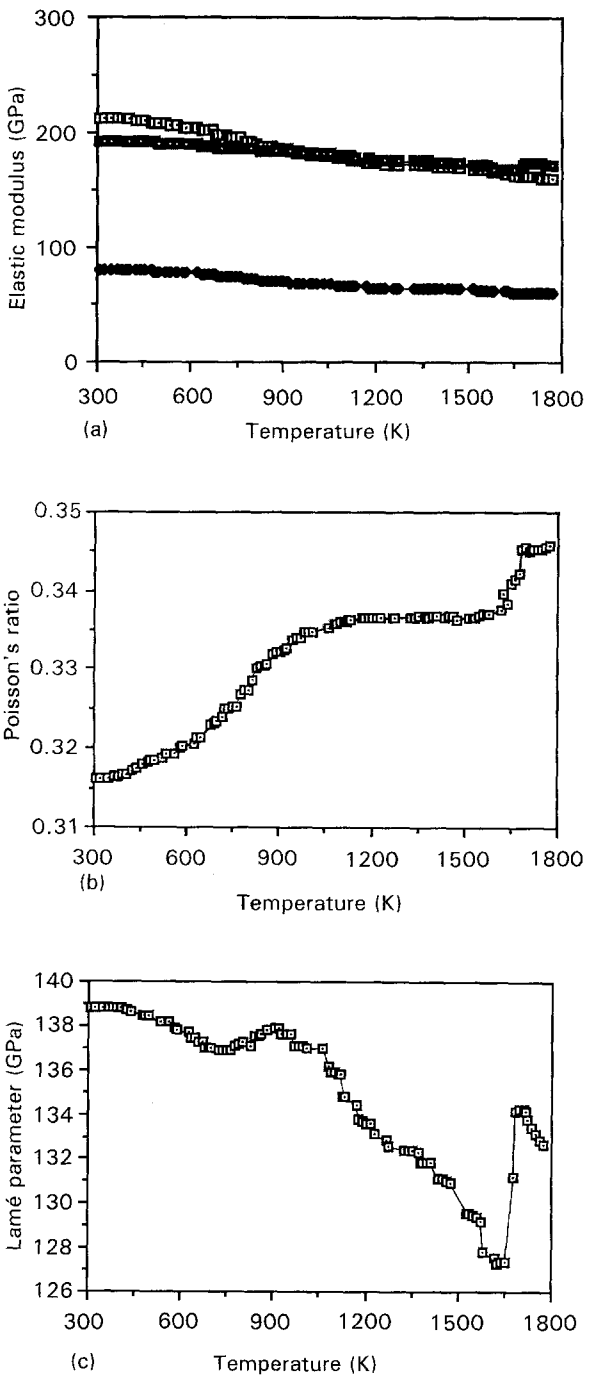

Figure 3 (a) (□) Young's, (◆) shear and (■) bulk moduli, (b) Poisson's ratio, and (c) Lamé parameter, of (Y)TZP as a function of temperature.

3.2. Temperature dependence of acoustic wave velocity anisotropy

In discussion of properties of materials it is useful to use an acoustic wave velocity anisotropy factor $\sqrt{3}V_t/V_l$ [28], where V_l and V_t are longitudinal and transverse wave velocity, respectively. The factor was calculated from room temperature to 1773 K, Figs 5–7 show the temperature dependence of the anisotropy for α-alumina, (Y)TZP and β′-sialon ceramics, respectively. Transverse wave velocity of alumina predominates over the longitudinal wave velocity in the room-temperature region, while the relation reverses in the elevated temperature range. The decimal fraction indicates inactivity of the dilational mode or activation of the shear mode in elastic solids. It would be the former, assumed from the relative decrease of the transverse wave velocity to the longitudinal wave velocity at high temperature. The longitudinal wave velocity of (Y)TZP exceeds the transverse wave velocity over the whole temperature range and the tendency is promoted with increasing temperature, suggesting activation of the shear mode. In sialon, there is no distinct anisotropy for acoustic wave velocity up to 1675 K, but the factor increases abruptly over 1675 K. This would be activation of the dilational mode due to binder components, assumed from the relative decrease of the longitudinal wave velocity to transverse wave velocity at high temperature.

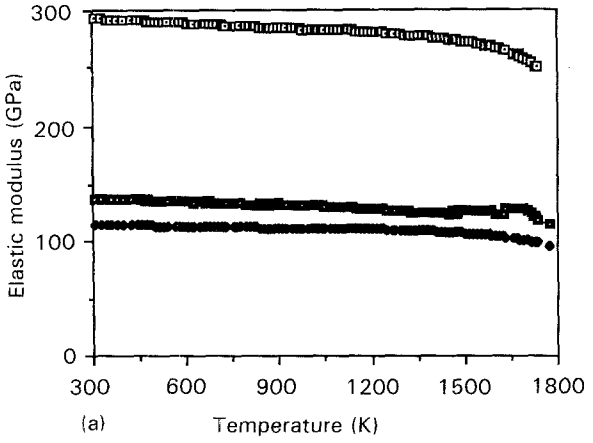

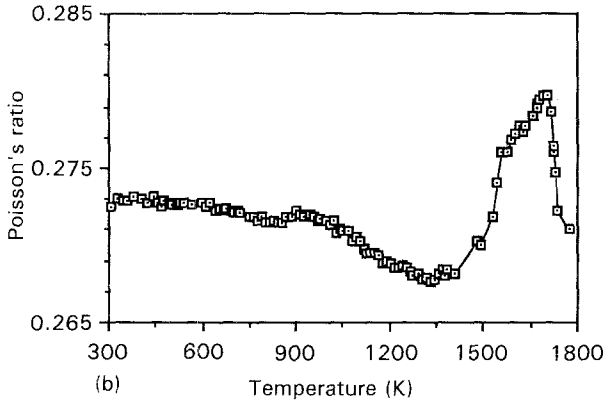

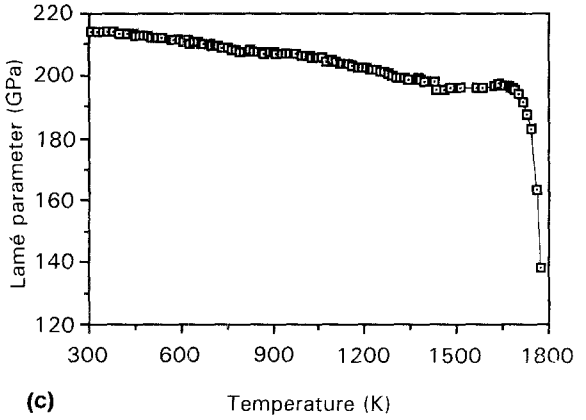

Figure 4 (a) ⊡ Young's, (◆) shear and (■) bulk moduli, (b) Poisson's ratio, and (c) Lamé parameter, of β′-sialon as a function of temperature.

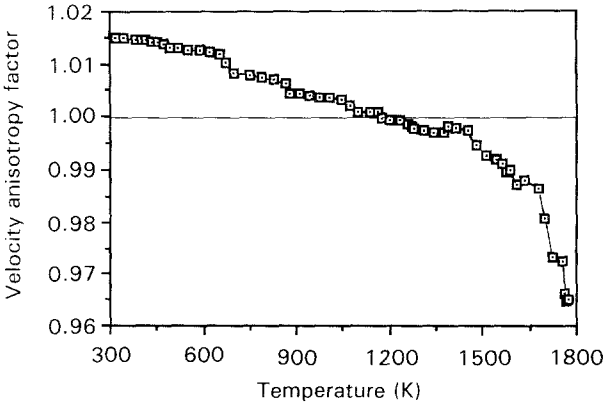

Figure 5 Acoustic wave velocity anisotropy factor versus temperature in α-alumina.

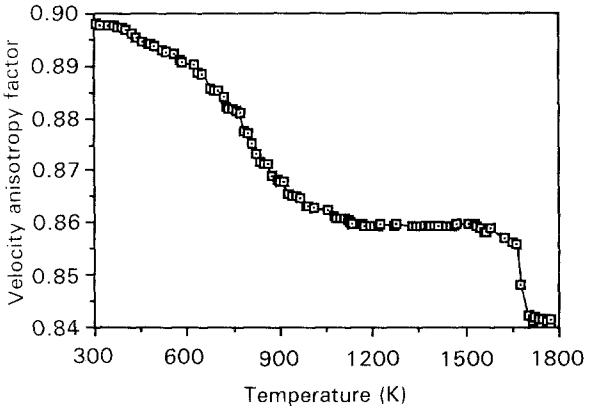

Figure 6 Acoustic wave velocity anisotropy factor versus temperature in (Y)TZP.

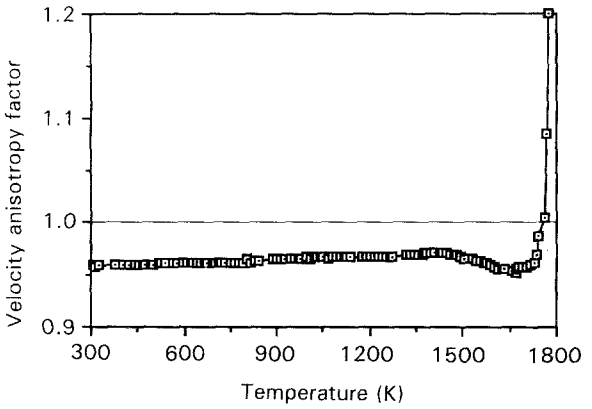

Figure 7 Acoustic wave velocity anisotropy factor versus temperature in β′-sialon.

3.3. Temperature dependence of internal friction

Internal friction curves for longitudinal and transverse waves of α-alumina, (Y)TZP and β′-sialon are shown in Figs 8–10, as a function of temperature. The temperature dependence of both curves for alumina resemble each other and they show a peak at around 1673 K. It is considered that these peaks correspond to softening due to the MgO binder. Both curves of (Y)TZP show large broad peaks at around 869 K, whereas the peak positions at elevated temperature differ from each other; the longitudinal wave friction increases suddenly from around 1570 K, while the transverse wave friction increases at around 1523 K and shows a peak at around 1650 K.The position of the low-temperature peak, the so-called "single relaxation peak" [2, 12], shifts to high temperature compared with the positions (at about 473 K) reported by Shimada *et al.* [2] and Sakaguchi *et al.* [3]. This can be explained by the frequency dependence of the internal friction peak temperature [12]. The reason for the occurrence of the low-temperature peak is unclear at the present time, although Shimada *et al.* [2] assumed two reasons, twin motion in monoclinic ZrO_2 or dislocation bowing resulting from the stress introduced by the flexural vibration. Internal friction curves of sialon reveal a gradual increase from around 1190 K for the longitudinal wave and an abrupt increase from around 1700 K for the transverse wave. This could

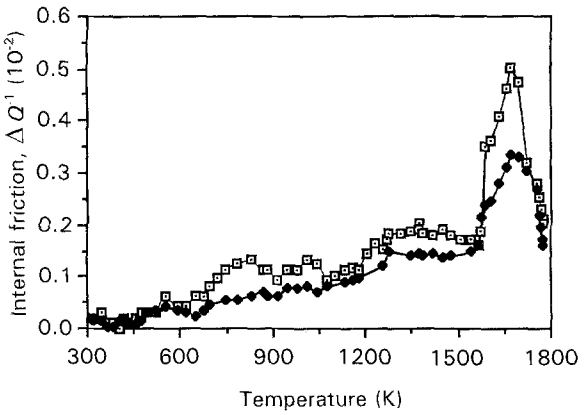

Figure 8 Temperature dependence of increased internal friction for longitudinal and transverse waves of α-alumina. (⊡) Dilational friction, (◆) shear friction.

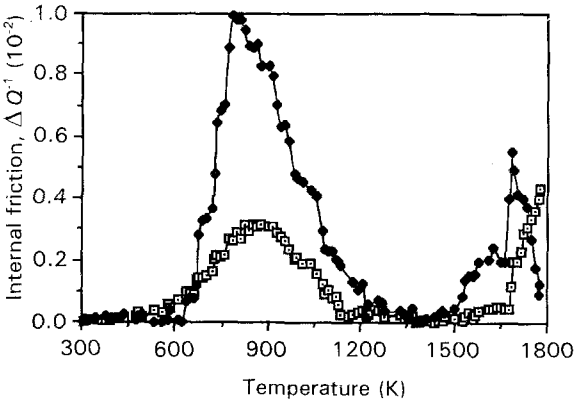

Figure 9 Temperature dependence of increased internal friction for longitudinal and transverse waves of (Y)TZP. (⊡) Dilational friction. (◆) shear friction.

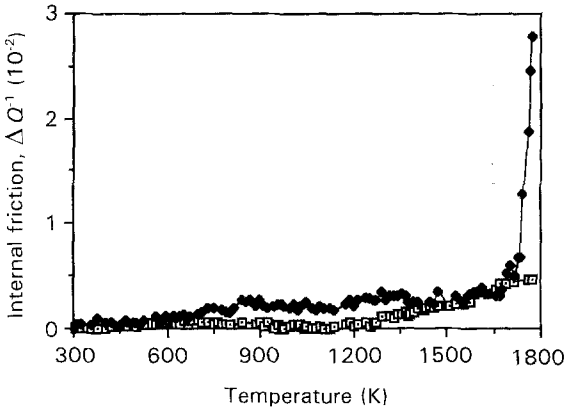

Figure 10 Temperature dependence of increased internal friction for longitudinal and transverse waves of β′-sialon. (⊡) Dilational friction, (◆) shear friction.

perhaps be the softening of the glassy phase of the grain boundary in sialon, as assumed from the results of Mosher and Raj [13].

4. Discussion

In propagation of an acoustic wave, acoustic energy generally decreases by absorption and scattering. The acoustic scattering effect plays an important part in the propagation for polycrystalline ceramics, especially at high temperature. Because the longitudinal wavelength of the β′-sialon, for example, is about 2 mm in a frequency of 5 MHz at room temperature, usage of the waveguide with threads of pitch 1.5 mm is effective for avoidance of spurious echoes in preliminary experiments. Thus we could determine spontaneously six elastic parameters (Young's, shear and bulk moduli, compressivity, Poisson's ratio, Lamé parameter λ), wave velocity anisotropy, longitudinal and transverse internal friction up to 1773 K. (However, as compressivity is the reciprocal of bulk modulus, figures of compressivity are eliminated in this study.)

Acoustic wave velocity which is mainly phonon velocity, varies with temperature and pressure due to non-harmonisity of potential between atoms. In the ultrasonic method, the pressure effect is negligible. All high-temperature elastic parameters obtained in this study show a sluggish decrease compared with those obtained by other methods such as flexural vibration [12] and resonance frequency methods [2, 3, 6, 7, 14, 15]. This would be due to the absence of a pressure effect in the ultrasonic method, because there is a possibility of deterioration due to high-frequency fatigue for other methods [19]. If the material is elastically isotropic, the anisotropy factor $A = 1$. The degree of anisotropy of certain cubic crystals is shown by the following values of A; iron 2.4; aluminium 1.2; copper 3.2; lead 4.0; NaCl 0.7; KCl 0.36; LiF 1.6 [28]. Three kinds of ceramic in this study show values near 1, especially in the room-temperature region, suggesting an apparently isotropic body.

The wave velocity anisotropy at room temperature not only depends on an intrinsic character of the materials, but also on grain-boundary orientation, preferential grain growth, residual stress and deformation mode. The temperature dependence for the boundary orientation and the grain growth in the three kinds of ceramics will be negligible in the elevated temperature range. As can be expected from the anisotropy curves of alumina and (Y)TZP in Figs 5 and 6, respectively, the effect of the residual stress and deformation mode decreases and changes, respectively, as temperature increases. Decrease in the anisotropy factors for the oxides in the high-temperature range suggests activation of the shear mode. However, sialon apparently shows activation of the dilational mode. This would be caused by absorption of the longitudinal wave due to the binder components, mainly consisting of oxides, as assumed from the gradual increase of internal friction for the longitudinal wave. It is known that diffusion of ions in the binder activates damping [6, 7, 13]. In order to evaluate accurately the high-temperature strength of materials, we must treat the acoustic wave velocity anisotropy as being connected to deformation mode or applied stress, taking into consideration high order elastic constants [29, 30].

The temperature dependence of Poisson's ratio for polycrystalline alumina [9] and fused silica [8] has been briefly reported, but no research work for various ceramics has been carried out on this subject. The increase in the ratios for alumina and (Y)TZP in the

high-temperature range, reflects the greater facility of relaxation by the shear process [31]. In the case of sialon, the occurrence of a peak at around 1670 K can be attributed to a large amount of binder (c.a 9 mass %), mainly consisting of yttria. Recovery of Poisson's ratio at around 1703 K indicates small deformability of the silicon nitride lattice in the high-temperature range. It is, therefore, expected that hot-pressed silicon nitride ceramics with a small amount of binder will have a larger shear resistance in the high-temperature range. The detailed results will be described in a subsequent paper.

As can be seen from Figs 8–10, the internal friction curves for longitudinal and transverse waves resemble each other for alumina, but differ for (Y)TZP and sialon; shear friction of (Y)TZP and sialon are more sensitive to relief of strain, as well as quartz [26], and softening of the glassy phase at grain boundaries [13], respectively, compared with the dilational friction. Relief of strain is related to superplasticity [17, 32]. Thus it is clear that simultaneous measurement of both dilational and shear friction values is an attractive method for accurate evaluation of high-temperature materials. In metals, particularly, this method would be extremely useful for studies of magnetism, recrystallization, solute solubility and grain growth, etc.

As assumed from elastic constant, C_{12}, in the elastic constant matrix, the Lamé parameter corresponds to the shear mode. The increase in the Lamé parameter of alumina in the high-temperature range apparently suggests inactivity of the shear mode. We cannot elucidate the reason, because the transverse wave velocity decreases at high temperature. In contrast, the high-temperature Lamé parameter is also sensitive to relief of strain for (Y)PSZ and diffusion of ions in the binder for sialon. Further work in this interesting area for ceramics is called for.

To obviate high-temperature ultrasonic couplant problems [33], in this study we used one body sample unified by the waveguide without the use of any couplant. However, the cost, scarcity of material and the difficulty of fabrication necessitates the use of a short or small specimen. A new technique will be described in a subsequent paper.

Acknowledgement

We thank Mr K. Yazawa, Managing Director, Choonpa Kogyo, for useful discussions.

Appendix. Equations for internal friction

Consider the echo diagram (Fig. A1) of wave propagation in a specimen with a waveguide.

1. Longitudinal wave internal friction

The echo amplitude of an ultrasonic wave at the bottom end of the waveguide at initial temperature, t_0, is represented as follows, using the continuity condition [34, 35] for amplitude

$$A_{l10} = P_l\{(S_1 - S_2) + S_2\}e^{-2\alpha_{l10}l_1} \quad \text{(A1)}$$

$$A_{l20} = P_l S_2 T e^{-2(\alpha_{l10}l_1 + \alpha_{l20}l_2)}, \quad \text{(A2)}$$

provided that

$$T = 1 - R^2 \quad \text{(A3)}$$

where A_{l10} and A_{l20} are echo amplitudes of the longitudinal wave from the shoulder and the specimen edge, respectively, α_{l0} attenuation coefficient per length at t_0, P_l the pulse sound pressure of the longitudinal wave, S_1 and S_2 the effective reflection area of the pulse wave at the shoulder and the specimen edge, respectively, and l_1 and l_2 the length of the waveguide and the specimen. T is the transmission coefficient for both ways, applying in the formula the reflection coefficient R_{12} in terms of the special acoustic impedences Z_1 and Z_2 for a particle displacement in a wave travelling from medium 1 to medium 2 [36]

$$R_{12} = \frac{Z_1 - Z_2}{Z_1 + Z_2} \quad \text{(A4)}$$

and assuming $R_{21} = -R_{12}$.

From equations A1 and A2

$$\frac{A_{l20}}{A_{l10}} = \frac{S_2 T e^{-2\alpha_{l20}l_2}}{S_1 - (1 - R)S_2} \quad \text{(A5)}$$

The equation at a given temperature, t, is

$$\frac{A_{l2t}}{A_{l1t}} = \frac{S_2 T e^{-2\alpha_{l2t}l_2}}{S_1 - (1 - R)S_2} \quad \text{(A6)}$$

where α_t is attenuation coefficient per length at t.

From Equations A5 and A6

$$\left(\frac{A_{l2t}}{A_{l1t}}\right)\Big/\left(\frac{A_{l20}}{A_{l10}}\right) = e^{-2(\alpha_{l2t} - \alpha_{l20})l_2} \quad \text{(A7)}$$

This is rewritten as

$$\alpha_{l2t} - \alpha_{l20} = -\frac{\left(\ln\frac{A_{l2t}}{A_{l1t}} - \ln\frac{A_{l20}}{A_{l10}}\right)}{2l_2} \quad \text{(A8)}$$

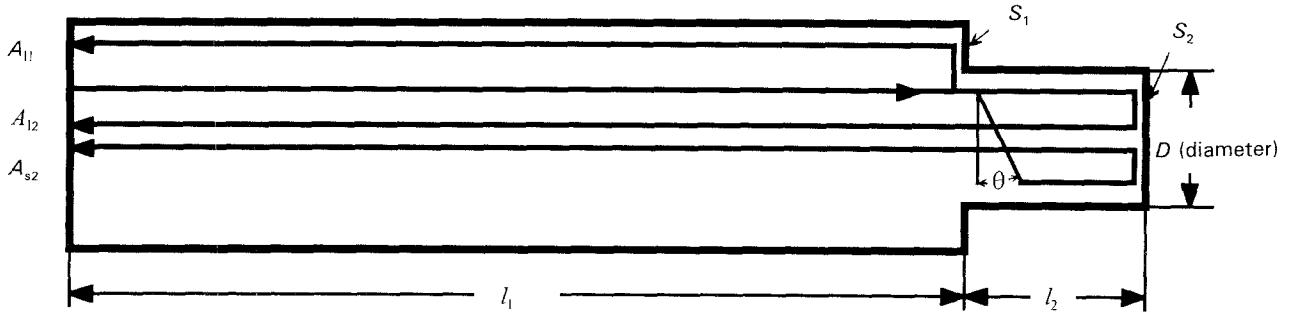

Figure A1 Echoes in the waveguide and specimen.

An amount of increase in attenuation per one wavelength in the range from t_0 to t, is described by

$$\Delta\alpha_{l2t}\lambda_{l2t} = (\alpha_{l2t} - \alpha_{l20})\lambda_{l2t} = (\alpha_{l2t} - \alpha_{l20})\frac{V_{l2t}}{f} \quad \text{(A9)}$$

where f is the frequency. Internal friction per one wavelength at t_0 gives

$$\begin{aligned} Q_{l20}^{-1} &= \frac{1}{2\pi}(1 - e^{-2\alpha_{l20}})\lambda_{20} \\ &\fallingdotseq \frac{1}{\pi}\alpha_{l20}\lambda_{l20} \\ &= \frac{1}{\pi}(\alpha_{l2t} - \Delta\alpha_{l2t})\lambda_{l2t} \end{aligned} \quad \text{(A10)}$$

The increasing rate in internal friction at t, due to the longitudinal wave can thus be represented as follows

$$\begin{aligned} \Delta Q_{l2t}^{-1} &= Q_{l2t}^{-1} - Q_{l20}^{-1} \\ &= -\frac{1}{\pi}\Delta\alpha_{l2t}\lambda_{l2t} \\ &= -\frac{1}{\pi}\left[\left(\ln\frac{A_{l2t}}{A_{l1t}} - \ln\frac{A_{l20}}{A_{l10}}\right)\right] \Big/ 2l_2 \\ &\quad \times \frac{V_{l2t}}{f} \end{aligned} \quad \text{(A11)}$$

2. Transverse wave internal friction

The echo amplitude of a transverse wave from the specimen edge at t is represented as follows

$$A_{s2t} = P_s S_2 T e^{-2\alpha_{l1t}l_1} e^{-(2l_2 - D\tan\theta)\alpha_{l2t}} e^{-D\alpha_{s2t}/\cos\theta} \quad \text{(A12)}$$

where A_{s2t} is the echo amplitude of the transverse wave from the specimen edge at t, P_s the pulse sound pressure of the transverse wave, D the diameter of the specimen, and θ the critical reflection angle.

Thus we can obtain

$$\left(\frac{A_{s2t}}{A_{s20}}\right) \Big/ \left(\frac{A_{l2t}}{A_{l20}}\right) = e^{D\tan\theta(\alpha_{l2t} - \alpha_{l20})} e^{-D(\alpha_{s2t} - \alpha_{s20})/\cos\theta} \quad \text{(A13)}$$

where

$$\sin\theta = \frac{V_{s2t}}{V_{l2t}} \quad \text{(A14)}$$

Equation A13 is rewritten:

$$\alpha_{s2t} - \alpha_{s20} = \sin\theta(\alpha_{l2t} - \alpha_{l20}) - \frac{\cos\theta}{D}\left(\ln\frac{A_{l2t}}{A_{l20}} - \ln\frac{A_{s2t}}{A_{s20}}\right) \quad \text{(A15)}$$

Attenuation per one wavelength is described by

$$\begin{aligned} \Delta\alpha_{s2t}\lambda_{s2t} &= (\alpha_{s2t} - \alpha_{s20})\lambda_{s2t} \\ &= (\alpha_{s2t} - \alpha_{s20})\frac{V_{s2t}}{f} \end{aligned} \quad \text{(A16)}$$

where V_{st} is the transverse wave velocity at t.

The increasing rate in internal friction at t due to the transverse wave can thus be represented as follows

$$\begin{aligned} \Delta Q_{s2t}^{-1} &= Q_{s2t}^{-1} - Q_{s20}^{-1} \\ &= \frac{1}{\pi}\Delta\alpha_{s2t}\lambda_{s2} \\ &= -\frac{1}{\pi}\left[\frac{\sin\theta}{2l^2}\left(\ln\frac{A_{l2t}}{A_{l1t}} - \ln\frac{A_{l20}}{A_{l10}}\right) + \frac{\cos\theta}{D}\left(\ln\frac{A_{s2t}}{A_{s20}} - \ln\frac{A_{l2t}}{A_{l20}}\right)\right] \\ &\quad \times \frac{V_{s2t}}{f} \end{aligned} \quad \text{(A17)}$$

Referernces

1. W. A. FATE, *J. Appl. Phys.* **46** (1975) 2375.
2. M. SHIMADA, K. MATSUSHITA, S. KURATANI, T. OKAMOTO, M. KOIZUMI, K. TSUKUMA and T. TSUKIDATE, *J. Am. Ceram. Soc.* **67** (1984) C-23.
3. S. SAKAGUCHI, F. WAKAI and Y. MATSUNO, *Yogyo-Kyokai* **95** (1987) 476.
4. T. D. GULDEN, *J. Am. Ceram. Soc.* **52** (1969) 585.
5. J. B. WACHTMAN, Jr and D. G. LAM Jr, *ibid.* **42** (1959) 254.
6. K. MATSUSHITA, T. OKAMOTO and M. SHIMADA, *J. Phys. Colloq.* **C10** (1985) 545.
7. J. B. WACHITMAN Jr, W. E. TEFFT, D. G. LAM Jr and C. S. APSTEIN, *Phys. Rev.* **122** (1961) 1754.
8. E. H. CARNEVALE, L. C. LYNNWORTH and G. S. LARSON, *J. Acoust. Soc. Am.* **36** (1964) 1678.
9. E. RYSHKEWITCH, *J. Am. Ceram. Soc.* **34** (1951) 322.
10. C. ZENER, *Phys. Rev.* **40** (1956) 906.
11. T. S. KÊ, *ibid.* **71** (1949) 533.
12. K. MATSUSHITA, T. OKAMOTO and M. SHIMADA, *J. Phys. Colloq.* **C10** (1985) 549.
13. D. R. MOSHER and R. RAJ, *J. Mater. Sci.* **11** (1976) 49.
14. S. SAKAGUCHI, N. MURAYAMA and F. WAKAI, *Yogyo-Kyokai* **95** (1987) 1219.
15. J. B. WACHTMAN Jr and W. E. TEFFT, *Rev. Sci. Instrum.* **29** (1958) 517.
16. J. F. W. BELL, *Philos. Mag.* **2** (1957) 113.
17. M. FUKUHARA, "Super High Strength Ceramics", in "Super Fine Ceramics", 19th Ceramic Lecture Meeting, September 1985, edited by K. Koumoto (Japanese Ceramic Society, Tokyo) p. 27.
18. M. FUKUHARA, *J. Am. Ceram. Soc.* **72** (1989) 236.
19. D. E. MACDONALD, *Eng. Fatigue Mech.* **8** (1976) 17.
20. N. P. CEDRONE, D. R. CURRAN, *J. Acoust. Soc. Am.* **26** (1954) 963.
21. R. L. FORGACS, *ibid.* **32** (1960) 1697.
22. A. SATHER, *ibid.* **43** (1968) 1291.
23. H. J. MCSKIMIN and E. S. FISHER, *J. Appl. Phys.* **31** (1960) 1627.
24. M. REDWOOD, "Mechanical Waveguides" (Pergamon Press, Oxford, 1960) p. 205.
25. H. IWASAKI, *J. Mater. Res. Soc. Jpn.* **30** (1981) 1044.
26. H. IWASAKI, *Ceramics (Jpn)* **12** (1977) 342.
27. K. TSUKUMA, private communication Apr. 1992.
28. C. F. SMITH and W. B. CRANDALL, *J. Am. Ceram. Soc.* **47** (1964) 624.
29. H. F. POLLARD, "Sound Waves in Solids" (Pion, London, 1977) p. 14.
30. D. S. HUGHES and J. L. KELLY, *Phys. Rev.* **92** (1953) 1145.
31. A. SEEGER and O. BUCK, *Z. Naturforsch.* **15a** (1960) 1056.
32. R. L. COBLE and W. D. KINGERY, *J. Am. Ceram. Soc.* **39** (1956) 377.
33. Y. KATSUMURA and M. FUKUHARA, in "Proceedings of the World Congress on High Tech Ceramics", 6th International Meeting on Modern Ceramics Technologies, Milan, Italy, June 1986, edited by P. Vincenzini (Elsevier, Amsterdam, 1987) p. 2735.
34. E. S. FISHER and C. J. RENKEN, *J. Acoust. Soc. Am.* **35** (1963) 1055.
35. R. B. LINDSAY, "Mechanical Radiation" (McGraw-Hill, New York, 1960) p. 74.
36. E. P. PAPADAKIS, *J. Appl. Phys.* **42** (1971) 2990.
37. E. P. PAPADAKIS, L.C. LYNNWORTH, K.A. FOWLER and E. H. CARNEVALE, *J. Acoust. Soc. Am.* **52** (1972) 850.

Received 27 April 1992
and accepted 24 February 1993